Colloid Polym Sci 275:537–545 (1997)

ORIGINAL CONTRIBUTION

C. Chevillard
M.A.V. Axelos

Phase separation of aqueous solution of methylcellulose

Received: 18 July 1996
Accepted: 17 February 1997

C. Chevillard · Dr. M.A.V. Axelos (✉)
INRA
Laboratoire de Physico Chimie
des Macromolécules
Rue de la Géraudière
BP 71627
44316 Nantes Cedex 02, France

Abstract As we determined visually by the temperature cloud point method, the coexistence phase curve of methylcellulose in aqueous solution belongs to the LCST (low critical solution temperature) type. Rheological dynamic measurements reveal the existence of three gel domains. The gel (I) localized in the homogeneous phase at low concentration and low temperature, is a very weak gel, where the cross-links are attributed to pairwise hydrophobic interactions between the most hydrophobic zones of the backbone: the trimethyl blocks. The second gel (II) was revealed in the high concentration regime and below the LCST, it may be attributed to the formation of crystallites which play the role of cross-linking points. The third gel was concomitant to the micro-phase separation. In these turbid gels, syneresis develops slowly with time: the higher the temperature and the lower the concentration, the faster the syneresis. Near the three sol–gel transitions, a power law frequency dependence of the loss and storage moduli was observed and the viscoelastic exponent $\Delta(G' \sim G'' \sim \omega^{\Delta})$ was found to be 0.76 and 0.8 and to reach 1 at high concentration.

Key words Methylcellulose – thermogelation – sol–gel transition – phase diagram – viscoelasticity

Introduction

Methylcellulose (MC), a water-soluble hydrophobically modified cellulose derivative, is a widely used polymer in a large number of industrial applications for its surfactant properties and unusual thermoreversible gelation upon increasing the temperature [1, 2]. The first field of application of methylcellulose was in food industries as a thickening, binding, suspending and emulsifying agent during food processing [3]. Methylcellulose is also well used in other fields for its adhesion properties (printing), moisture retention (film), adsorption properties (stabilization of paint) and thermothickening ability (cosmetics, pharmaceuticals) [4].

Cellulose is insoluble in water because of a large number of intermolecular hydrogen bonds which stabilize a fribrillar tertiary structure with a high order of crystallinity. Due to the substitution of some OH groups of the anhydroglucose units by hydrophobic groups (CH_3), methylcellulose becomes soluble in cold water, which may be attributed to an increase of the hydrogen bonding between the water molecules and the oxygen of the remaining hydroxyl functions of the polymer. Methylcellulose is characterized by the average degree of substitution (DS) which is defined as the average number of hydroxyl groups substituted per anhydroglucose. This parameter masks the fact that commercial methylcelluloses have a heterogeneous substituent distribution

Colloid & Polymer Science, Vol. 275, No. 6 (1997)

along their backbone induced by the industrial process of preparation [5]. The presence of such a distribution of the CH_3 groups must lead to a decrease in the hydration [6, 7] of some parts of the chain when an increasing temperature induces hydrophobic interactions, thus allowing an entropically driven polymer–polymer association in these highly derivatised areas of the polymer, the so-called "micellar gels" introduced by Rees [8].

The gel, obtained by heating, is associated with phase separation. This polymer displays a lower critical solution temperature (LCST) [9]. Below the LCST the solution is a one-phase system. Above this temperature the solution becomes cloudy and the gel formation prevents from a complete phase separation leading to a homogeneous white phase. At a very high polymer concentration methylcellulose is able to crystallize [10]. This co-occurence of the sol–gel transition and two-phase separation have already been reported for a large number of polymeric solutions in which the thermodynamic quality of the solvent is reduced by temperature or in which the solvent composition changes. Depending on the polymer–solvent systems the gel formation has been attributed to spinodal decomposition (the origin of the network being the connectivity between the polymer-rich phase) or to crystallization, or to a manifestation of both crystallization and spinodal decomposition [11–13].

This work approaches an aqueous solution of MC differently from what has already been done in the past. This system was often studied by a temperature sweep in the biphasic region [1, 2, 9, 14, 15]. But few data exist near the equilibrium state because of a slow kinetic of association which depends on the temperature and polymer concentrations. For this reason we have undertaken a systematic series of studies as close as possible to the thermodynamic equilibrium in order to establish the phase diagram (binodal curve) and to describe the rheological behavior.

Experimental

Sample

The methylcellulose which was used is Methocel A4C from the Dow Chemical Company. As specified by the producer the methoxyl content is between 27.5 and 31.5%, leading to an average DS of 1.8. The intrinsic viscosity we measured in water at 25 °C was 4.5 dl/g. The average distribution of the methoxyl groups per monomer unit is 10% of non-substituted monomers, 29% of mono-substituted monomers, 39% of di-substituted monomers and 22% tri-substituted monomers as measured by Vigouret [14]. An average number of 3 carboxyl groups per 1000 monomers have also been detected by conductimetry.

Sample preparation

Prior to use the commercial sample was purified by extensive dialysis against distilled water using 8000 Da cutoff cellulose membranes and then lyophilized. Purified methylcellulose was dissolved in cold (5 °C) distilled water under vigourous stirring for up to 12 h. The solution was centrifuged at 15000 g during 1 h at 5 °C in order to precipitate some insoluble particles. The supernatant, always at 5 °C, is filtered on 0.2 μm sterilized filters in cellulose acetate (Minisart SM16534K) for solutions with a concentration less than 10 g/l and on 0.45 μm (Minisart SM16555K) for solutions between 10 and 25 g/l. Because of the heating treatment applied afterwards, solutions were degassed under vacuum.

The more concentrated solutions ($C > 30$ g/l) were prepared by rehydrating the lyophilized product at 5 °C for 3 days. The viscous solution thus obtained was centrifuged as indicated above but not degassed.

Measurements

Cloud point determination

Solutions at 5 °C contained in stopped cylindrical cells were heated in a thermostated bath to the required temperature. As the process of separation can be very slow, tubes were left in the bath for about one week at each temperature. The onset of the appearance of slight turbidity was visually determined by comparison with a tube of the cold solution at the same concentration. After these observations the bath temperature was increased and the process was repeated. The cloud point temperature we have determined in this way corresponds in fact to the temperature for which about 95% of the light is transmitted as checked on a spectrophotometer at 600 nm.

Optical density measurements

Light-transmitted measurements were made at 600 nm on a Lambda 2 Perkin Elmer spectrophotometer with a water-jacketed cell holder coupled with a Haake circulating bath. Temperatures were maintained at a fixed value to determine the kinetics of the phase separation or automatically ramped by a temperature controller/programmer. The time or temperature at the cloud points were taken as previously explained when 95% of the light is transmitted.

Viscoelasticity measurements

Oscillatory shear measurements were performed using a Contraves Low Shear 40 and a CarriMed CS 50 rheometer according to the concentration and temperature of the sample. The first one is a shear-rate imposed, very sensitive, temperature-regulated, couette rheometer which can measure torque in the range 10^{-3} mN m to 10 mN m ($R_1 = 6$ mm, $R_2 = 6.5$ mm, $h = 18$ mm). It has been used to determine the rheological properties in the one-phase domain of the phase diagram and for polymer concentrations less than 20 g/l. The second one is a controlled-stress rheometer fitted with a cone-plate device (radius 20 mm, cone-plate angle 4°). The temperature is controlled by the Pelletier effect which allows rapid changes in temperature. The cone is linked to a stress-controlling device that adjusts the torque necessary to maintain an imposed strain. This rheometer has been used for polymer concentrations larger than 25 g/l to study the rheological behaviour at different temperatures crossing the binodal curve.

The methylcellulose solution, initially at 5 °C, was put in the rheometer which was previously thermostated at the final desired temperature in the case of the Contraves, or at 5 °C with the Carri-med and then heated rapidly in situ. A layer of paraffin oil was added to protect the sample from dehydration. One first runs a time sweep at a fixed frequency, ω, to control the kinetics and then performs a frequency sweep, between 10^{-2} and 5 Hz, to get a mechanical spectrum: $G'(\omega)$ and $G''(\omega)$, the storage and loss modulus, respectively. The strain was fixed at 10% on the Contraves and 5% on the Carri-med; both these values are in the linear regime of the samples under study.

Results

Phase diagram

The concave shape of the cloud point curve temperature-concentration thus obtained by our procedure (Fig. 1) indicates that methylcellulose in water exhibits a lower critical solution temperature (LCST). Below this curve the system was clear and homogeneous, and above it turned into a homogeneously turbid gel. This phenomenon is largely used in industry to obtain a thermothickening effect. Only at a high temperature and low concentration it was possible to obtain a complete phase separation.

All these systems are out of the equilibrium and evolve differently depending on the temperature and polymer concentration. We prepared five test tubes of aqueous solution of MC at different concentrations (1.9, 4.8, 9.9, 15.0, 24.6 g/l) and set them at 67 °C for the entire

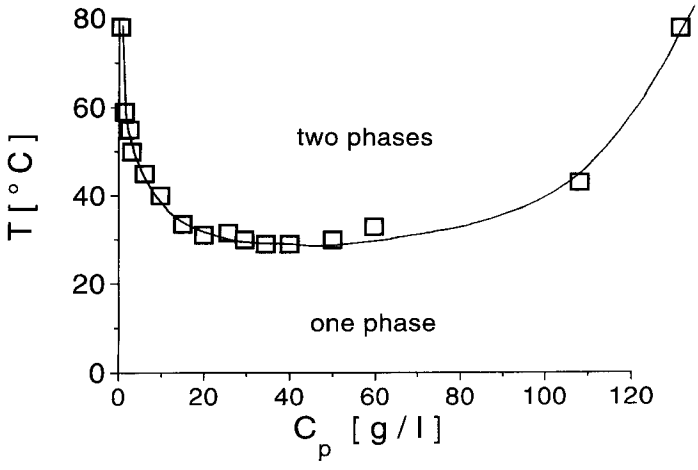

Fig. 1 Cloud point as a function of the methylcellulose A4C concentration in water

duration of the observation. We controlled the turbidity by visual observation and the physical aspect of the samples by tilting the test tubes. After one hour the test tube (1.9 g/l) closest to the cloud point curve was weakly turbid and ran. The four other concentrations had all the same aspect of a strong turbid gel. After one week the concentration 4.8 g/l began to develop a syneresis. After two weeks, as the test tube at the concentration 4.8 g/l continued to evolve, the concentration 9.9 g/l started out a syneresis as well. After two months the concentration 1.9 g/l was the same as it was at the start, the syneresis in 4.8 g/l was complete, it was widely advanced in 9.9 g/l, just starting out in 15 g/l, and still non-existent in 24.6 g/l. By increasing the temperature, the process of phase separation is accelerated, and the system evolved rapidly to a complete phase separation, in less than 10 days (1 g/l, 80 °C), with a precipitate less turbid than previously obtained. The system was then in a state of equilibrium, and the points defined by the respective concentration in each phase belonged to the binodal curve and in good agreement with the cloud point curve. The method which was used for measuring the cloud point temperature allows us to say that the curve thus obtained could be identified with the binodal curve. Indeed the cloud point temperature determined by our procedure is considerably smaller than the one obtained, as usual, by temperature sweep. As we were able to verify, at a polymer concentration of 26 g/l with a temperature sweep as low as 0.016 °C/mn, the cloud point was 38 °C instead of 31.5 °C according to the method described above.

From the minimum in this curve we determined a critical temperature $T_c = 29 \pm 2$ °C and a critical polymer concentration $C_c = 45 \pm 5$ g/l. It was possible to estimate the molecular weight, M_W of the sample, by using the

Colloid & Polymer Science, Vol. 275, No. 6 (1997)

critical concentration determined from the phase diagram. From the Flory–Huggins theory [16] the molecular weight is related to the critical point in the following equation,

$$M_W = \frac{m_0^3}{(C_c v_{sp})^2},$$

where m_0 is the molecular weight of the monomer (taking into account the degree of substitution, $m_0 = 186$ g/mol), and v_{sp} is the specific volume, $v_{sp} = 133\ cm^3/mol$ [7]. The molecular weight thus obtained, $M_W = 180\,000 \pm 50\,000$ g/mol, corresponds with the molecular weight given by Sarkar $M_W = 140\,000$ g/mol [2] and that obtained recently by Hirrien [17] from viscometric measurements: $M_v = 149\,000$ g/mol.

The sol–gel transition at low temperature, between 2–20 g/l (gel I)

In the one-phase region, weak gels were visually observed for polymer concentration, around 10 g/l, and for temperature below 30 °C. In order to accurately determine the sol–gel transition, oscillatory shear measurements were made in the clear phase at different concentrations lower than 20 g/l and at different temperatures.

All the mechanical spectra were recorded when a constant value in the storage G' with time was reached at a given frequency. In the one-phase region, no evolution of G' was found beyond 20 min. The Fig. 2 displays a series of mechanical spectra of a sample at the concentration 9 g/l and at different temperatures (5, 15, 30, 50 °C). At 5 °C the storage modulus $G'(\omega)$ increased like ω^2 whereas the loss modulus $G''(\omega)$ increased like ω^1 in the domain of frequencies explored as expected for a pure viscous solution. At 15 °C, $G'(\omega)$ initiated a plateau at low frequencies in the range observed, and cut $G''(\omega)$ at G_x at a cross-over frequency ω_0. As the temperature increased, G' increased and ω_0 went to higher frequencies. We reported G_x with respect to ω_0 in Fig. 3 and found that G_x follows a power law of ω_0 with an exponent Δ equal to 0.76 ± 0.04:

$$G_x(\omega_0) = G'(\omega_0) = G''(\omega_0) \sim \omega_0^{\Delta}.$$

We rescaled all mechanical spectra for temperatures less than 30 °C, using as reduced variable G^*/G_x and ω/ω_0. The master curve thus obtained (Fig. 4) displays a constant value for $\omega \ll \omega_0$ while for $\omega \gg \omega_0$ both G' and G'' scale

Fig. 2 Mechanical spectra for 9 g/l methylcellulose solution at different temperatures: (a) 5 °C, (b) 15 °C, (c) 30 °C, (d) 50 °C, G' ■, G'' □

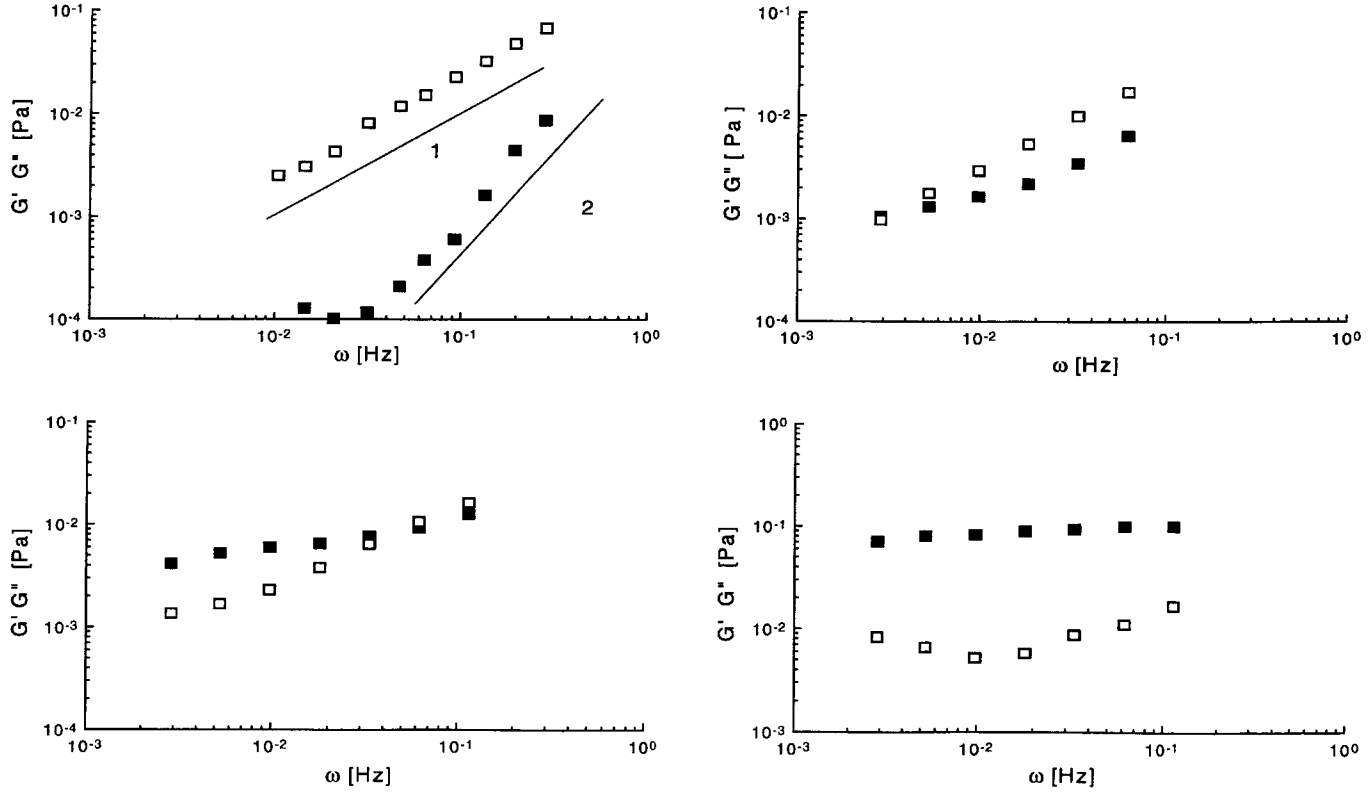

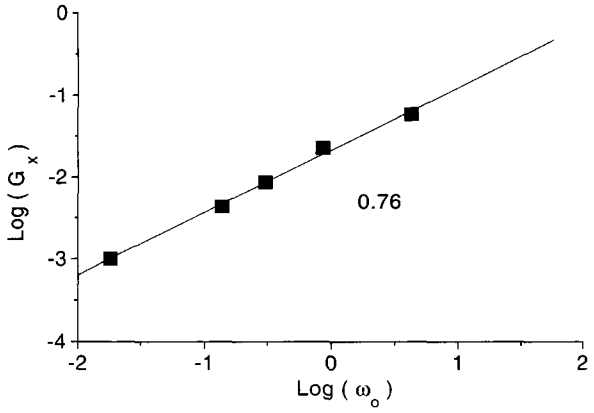

Fig. 3 Shear modulus $G_x = G'(\omega_0) = G''(\omega_0)$ with respect to the cross-over frequency ω_0. The straight line has a slope $\Delta = 0.76 \pm 0.04$

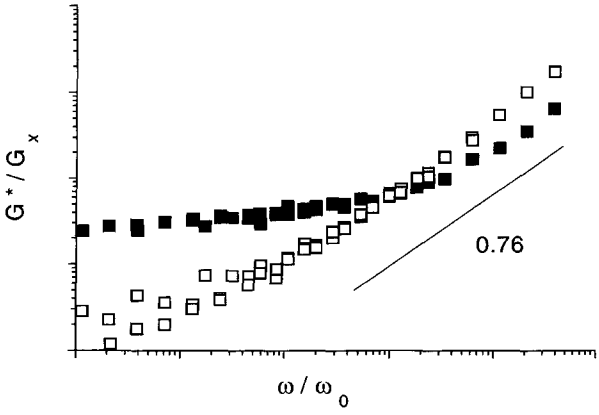

Fig. 4 Data collapse G'/G_x (■) and G''/G_x (□) versus ω/ω_0, from oscillatory measurements above the gel point (Log–Log). For $\omega > \omega_0$, G' and G'' scale as $\omega^{0.76}$

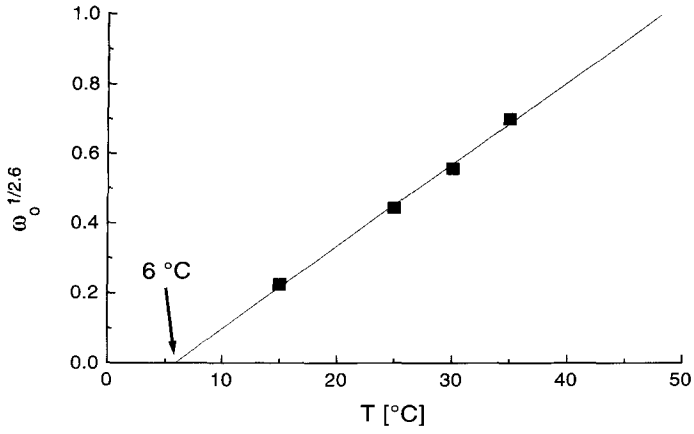

Fig. 5 Evolution of the cross-over frequency with the temperature just above the sol–gel transition for methylcellulose at 9 g/l. Determination of the exponent z: $z = 2.6 \pm 0.1$ and the sol–gel temperature: $T_g = 6\,^{\circ}C \pm 1$

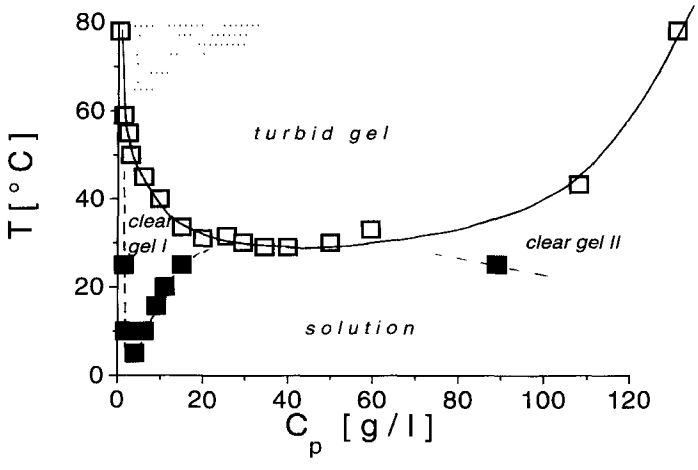

Fig. 6 Phase diagram of methylcellulose of A4C including the cloud point curve (□) and the sol–gel line ■ determined from oscillatory measurements. The clear gel I is a weak gel which is obtained after a few minutes, whereas the clear gel II is a stronger gel obtained after a few days of ageing. The hatch domain is a complete phase separation after two months

with almost the same exponent 0.76 as found before. Moreover, we determined the sol–gel temperature, T_g, at this polymer concentration, from the evolution of ω_0 with the temperature. We expected ω_0 to obey a power law behaviour: $\omega_0 \sim ((T - T_g)/T_g)^z$ and thus plotting $\omega_0^{1/z}$ against T and adjusting z for the best straight line fit determined $z = 2.6 \pm 0.2$ and yielded an estimate for $T_g = 6\,^{\circ}C \pm 1$ (Fig. 5).

The exponents Δ and z thus obtained are close to values obtained by some authors in others gelling systems such as silicon alkoxide [18], pectin [19], polyoxypropylated trimethylolpropane [20], and the gelation process, thus revealed, was described in terms of the percolation process [21]. A consequence of this theory is the rheological behaviour at the gel point with $G''/G' = \tan(\Delta\pi/2)$ whatever the frequency range. Most of the time this critical point is tricky to obtain, which is why we decided to overestimate the temperature of the sol–gel transition, considering that the rheological signature of the transition was when $G'(\omega)$ cut $G''(\omega)$ at $\omega_0 = 0.003$ Hz. The sol–gel temperature thus determined, for different polymer concentrations, is reported on the phase diagram in Fig. 6.

In the weak concentration domain, the gel phase disappeared below 1.5 g/l, whatever the temperature. Because of the very weak value of G^* this limit was difficult to detect

with the method described above. We have assumed in this case that the sol–gel transition was given by the onset of a non-Newtonian behavior in the flow curve with an increase of the apparent viscosity as the shear rate decreased.

The sol–gel transition at low temperature and high concentration (gel II)

At a high polymer concentration, the gelation is a time-dependent process which is very slow. Conversely, to gel I, the kinetics seem to be infinite and the final stage was still not reached by the end of one week. For six days, by oscillatory shear measurements, we followed the ageing of a sample at 89 g/l and at a constant temperature, 25 °C (Fig. 7). The first spectrum recorded when the temperature reached 25 °C indicated that the system was already a gel in the sense defined above (gel I). As time goes on, the storage modulus $G'(\omega)$ increased steadily and cut the loss modulus $G''(\omega)$, at higher and higher frequencies, finally reaching above G'' in the frequency range observed (Fig. 7). Behind the frequency sweep, a creep experiment was necessary to assert that the system was a viscolelastic solid (inset of Fig. 7). As it was previously done in the gel I domain we reported G_x with respect to ω_0 and found that the exponent Δ was equal to 1 ± 0.01 (Fig. 8).

It must also be mentioned that at a polymer concentration higher than 100 g/l we have observed the presence of small white particles after one week of ageing at 25 °C. The number of these particles visibly increased with the temperature.

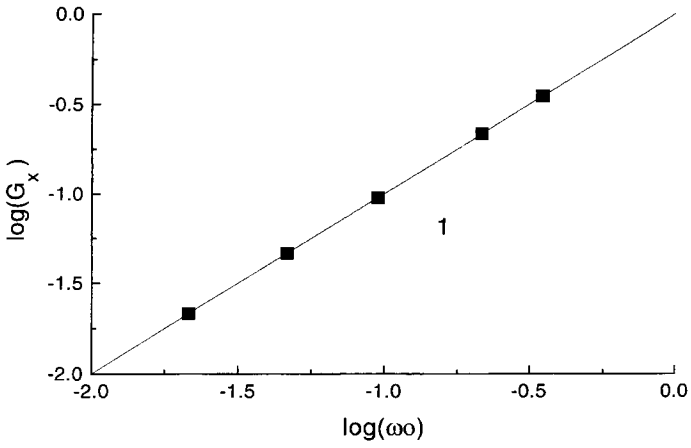

Fig. 8 Shear modulus $G_x = G'(\omega_0) = G''(\omega_0)$ with respect to the cross-over frequency ω_0. The straight line has a slope $\Delta = 1 \pm 0.01$

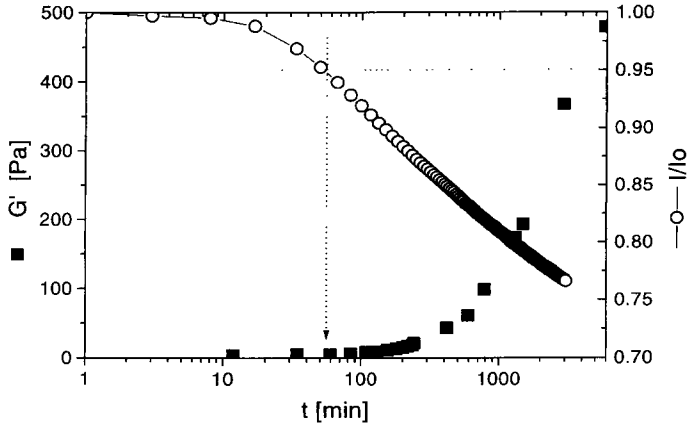

Fig. 9 Evolution of the transmittance (○) and the storage modulus G' (■) at $\omega = 0.01$ Hz, with respect to the time for methylcellulose A4C, 89 g/l at 25 °C. The cloud point defined for a transmittance of 0.95 as it is indicated by the arrow

Fig. 7 Mechanical spectrum for methylcellulose A4C, 89 g/l, after 6 days of ageing at 25 °C (G' ■, G'' □). The inset of the figure presents a creep experiment done after the frequency sweep at a shear stress 5 N/m²

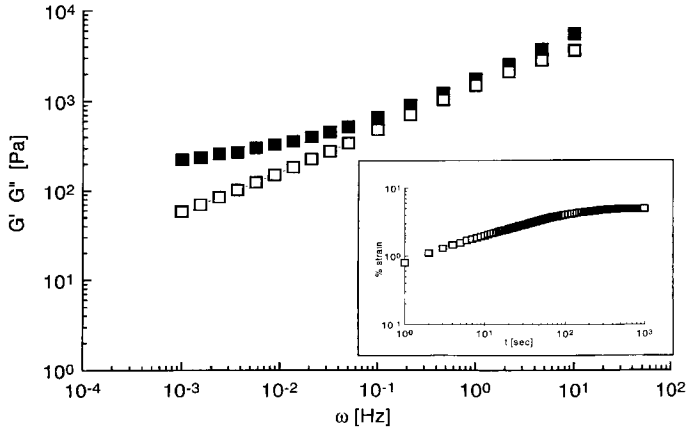

The sol–gel transition in the two-phase domain

Oscillatory shear measurements and turbidity measurements were carried out, for four days, on a sample at 60 g/l and 40 °C. This temperature, 10 °C above the binodal curve, was choosen in order to accelerate the phenomenon from several weeks, which was the time necessary to obtain the cloud point temperature, to a few days. And at this temperature the time of measurement was still small enough in comparison with the evolution of the system.

In Fig. 9 we reported the transmittance versus the time and the storage modulus G' measured at $\omega = 0.01$ Hz. We noticed that, the increasing of G' was not stabilized after

4 days, and the start of this growth coincided with the appearance of the turbidity, according to the criterion used for measuring the cloud point temperature, that is to say 95% of the transmitted light. As previously observed on the mechanical spectra recorded during the sol to gel transition, $G'(\omega)$ cut $G''(\omega)$ at a cross-over frequency which increased with time. During the first 6 h of ageing it was found that G_x follows a power law like $\omega_0^{0.8}$.

The same types of experiment, done for a sample at 20 g/l and 40 °C, confirmed the previous one, that is to say the turbidity and the gelation process are closely linked.

Evolution of the storage modulus with the temperature at low polymer concentration

At a fixed concentration of 9 g/l and frequency of 0.005 Hz, the storage modulus G'_0 was measured with respect to the temperature. In the clear gel I phase, the values of G'_0 were the final value at the end of the kinetics, whereas for temperature above the LCST, the values of G'_0 were taken after 1 h because the kinetics was infinitely long. As shown in Fig. 10, G'_0 versus temperature can be described by two ascending straight lines. The first one, with a slight slope, corresponds to the clear gel I. The second one, with a steeper slope, corresponds to the turbid gel. Therefore the large increase of G'_0 above 35 °C is related to the important structural change induced by the phase separation. It must be pointed out that the two transition temperatures determined through the evolution of G' versus temperature at low frequency corresponds to the results obtained previously on the sol–gel and the one-phase/two-phase transition temperatures.

Fig. 10 G' at 0.005 Hz versus T for methylcellulose A4C at 9 g/l

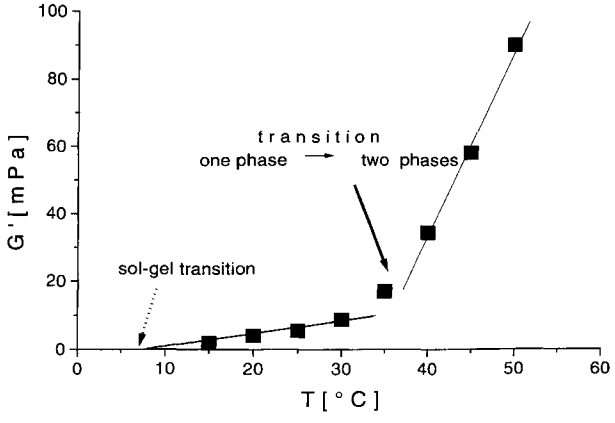

Reversibility in temperature

The aqueous solution of methylcellulose is thermoreversible, which is easy to observe visually through the turbidity. This was also observed on rheological measurements. The mechanical spectrum, of a sample at 15 g/l, 25 °C, was the same as if it was carried to and held at 45 °C during 6 h, then quenched at 25 °C and held at this temperature during 6 h. This experiment points out again the importance of the ageing time in the observation of the reversibility of this system. The hysteresis effect, as reported very often in literature [2, 14, 15], should disappear if the equilibrium was reached at each temperature step.

Reversibility in concentration

We prepared, as usual, a sample at a concentration of 15 g/l, carried to 25 °C and held at this temperature. Then on an aliquot we checked that the mechanical spectrum corresponded to a system at the sol–gel transition. The sample at 15 g/l was then diluted to 5 g/l with distilled water at 25 °C. The mechanical spectrum obtained was of gel-type. On the way back we forced the system to cross the transition by concentrating the sample to 22.9 g/l at 25 °C with a rotavapor. The rheological answer was characteristic of a liquid thus implying that this system displays a gel → sol transition by increasing the concentration.

Discussion

Methylcellulose displays a LCST as expected for polymers that exhibit a dual affinity of the polar hydrophilic group and the nonpolar hydrophobic group of the polymer towards the solvant. Similar phase separation phenomena have been described for other cellulose derivatives such as (Hydroxypropyl) cellulose [22] and ethyl (hydroxylethyl) cellulose [23] or for synthetic polymer such as copolymer of ethylene oxide and propylene oxide [24]. But the key feature of methylcellulose is the ability to form gels when heated. Gelation always occurs when a connected structure spans the entire sample, giving rise to a solid-like viscoelastic behavior. Depending on the polymer structure and the thermodynamic conditions, the associative elements, or crosslinks, may vary.

Commercial methylcellulose is known to display a heterogeneous substituent distribution of the methyl groups along their cellulose backbone [5] leading to heavily as well as poorly modified zones. In other words, the commercial methylcellulose cannot be considered to be a random copolymer but rather a complex block of copolymers. In this framework, the sol–gel transition of percolation

type which we revealed at a low polymer concentration by increasing the temperature (gel I), could be explained by the association, along the polymer backbone, of the most hydrophobic regions. For such a mechanism we expect that the number and length of crosslinks increase with temperature. At a higher temperature another mechanism comes into play which leads, in principle, to phase separation. The concomitance of the formation of a gel and the growth of polymer-rich microdomains, as shown in Fig. 9, prevent a phase separation from occurring but leads instead to a turbid gel, which may be interpreted as a microphase separation. This turbid gel is a metastable state and will end to collapse and excrete the solvant all the more easily as the temperature is high and the concentration is low, as it was observed in the experiments which were done at 67 °C for increasing polymer concentrations. The heterogeneous distribution of the methyl groups along the backbone seems to be essential to obtain the turbid gel since the aqueous solution of homogeneous methylcellulose displays precipitation, or classical phase separation, instead of gelation [25, 26]. Moreover, X-ray diffraction patterns obtained by several authors on methylcellulose turbid gels, support the fact that crystallites of trimethyl glucose are present [10] and operate as cross-links [27]. A chain which took part in the forming of a cross-link, is itself trapped in other cross-links giving rise to a gel. In this way the mobility of the chains is reduced and the phase separation process considerably slowed.

At a higher polymer concentration another sol–gel transition took place in the one-phase domain (gel II). Investigations in this part of the phase diagram were too sparse to draw out a non-equivocal explanation. Nevertheless, the process of gelation, which develops over very long time, may also be reasonably attributed to the formation of the same type of crystallites since no difference in X-ray diffraction patterns was observed between turbid gels and the powder at room temperature [10].

Between both gel domains the liquid-like response of the sample between 20 and 80 g/l and for temperatures lower than 30 °C is quite puzzling. Our interpretation of the above results is that in (gel I) the cross-linking will result in the association of only two polymer chains by their trimethyl glucose block. At a constant temperature, the increase of the polymer concentration will favour the association of the most hydrophobic zones between themselves in bundles instead of pairs. In this way the overall connectivity will disappear leading to a solution of aggregates. At a higher concentration the connectivity between the aggregates is again possible, leading to a gel (gel II) and the bundles will lead slowly to the crystallite formation.

The three sol–gel transitions of percolation type observed through oscillatory shear measurements are characterized by the scaling relation: $G^*(\omega) \sim \omega^{\Delta}$. Without going into detail in the study of the variation of Δ a with polymer concentration [28, 29] we want to mention that the exponent Δ was found to be almost the same ($\Delta = 0.76$ and $\Delta = 0.8$) when the concentration is low enough to follow the transition from the beginning of the increase of G' in the low frequency range. At a higher concentration it was not possible to follow the onset of the transition, and we suggest that the value $\Delta = 1$ obtained may be ascribed to the fact that the system was immediately far from the percolation transition. The clue to our interpretation is the existence of inter-chain associations between sequences of highly methylated monomers whose structure will vary with the polymer concentration. These "hydrophobic clusters" would allow linking two polymer chains at a low concentration giving rise to a weak gel, while bundles, which act as nuclei, would be predominant as the concentration increases. Thus the phase separation process which leads to the building up of strongly concentrated microdomains will also favor crystallite formation. This role played by the phase separation has also been shown in the case of physical gels linking through crystallites arising from hydrogen bonds such as agarose [30]. The dominant role of hydrophobic interactions, and their strength which depends on the local structure of the hydrophobic zones in the process of methylcellulose gelation, is very similar to what has been observed for polypeptide [31]. Moreover, the binding of an anionic surfactant observed on methylcellulose leading to the vanishing of aggregates [32] or gel I [33] reinforced this interpretation.

Acknowledgments This present work was supported by the French CNRS-PIRMAT program. The financial assistance of Rhone-Poulenc is also gratefully acknowledged. We thank Professor JF Joanny (ICS Institut Charles Sadron, Strasbourg), Dr. M. Kolb (ENS Ecole Normale Supérieure, Lyon) and L. Leibler (Unité de Recherche Mixte CNRS Elf-Atochem, Paris) for the interest they have shown in this project, and for their enlightening discussions. We are also indebted to Dow France for providing the methylcellulose A4C sample.

References

1. Heymann E (1935) Trans Farad Soc 31:846–864
2. Sarkar N (1979) Appl Polym Sci 24: 1073–1087
3. Grover JA (1986) In: Glicksman M (ed) Food Hydrocolloids, Vol III, CRC Press, Boca Raton, pp 121–154
4. Greminger GK, Savage AB (1959) In: Whistler RL, BeMiller JN (eds) Industrial Gums-Polysaccharides and their derivatives. Academic Press, New York, pp 565–596

5. Arisz PW, Kauw HJJ, Boon JJ (1995) Carbohydr Res 271:1–14
6. Doelker E (1990) Stud Polym Sci 8: 125–145
7. Koda S, Hori T, Nomura H, Kawaizumi F (1991) Polymer 32:2806–2810
8. Rees DA (1972) Chem Ind London 630
9. Sarkar N (1995) Carbohydr Polym 26:195–203
10. Khomutov LI, Ryskina II, Panina NI, Dubina LG, Timofeeva GH (1993) Polym Sci 35:320–323
11. Kawanishi K, Komatsu M, Inoue T (1987) Polymer 28:980–984
12. Palma-Vittorelli MB (1989) Int J Quantum Chem 35:113–124
13. Matsuo M, Kawase M, Sugiura Y, Takematsu S, Hara C (1993) Macromolecules 26:4461–4471
14. Vigouret M, Rinaudo M, Desbrières J (1996) J Chim Phys 93:858–869
15. Haque A, Morris ER (1993) Carbohydr Polym 22:161–173
16. Flory PJ (1978) Principles of Polymer Chemistry. Cornell University Press, Ithaca and London
17. Hirrien M, Desbrières J, Rinaudo M (1996) Carbohydr Polym, in press
18. Devreux F, Boilot JP, Chaput F, Malier L, Axelos MAV (1993) Phys Rev E 47:2689–2694
19. Axelos MAV, Kolb M (1990) Phys Rev Lett 64:1457–1460
20. Durand D, Delsanti M, Adam M, Luck JM (1987) Europhys Lett 3:297–301
21. Stauffer D (1985) Introduction to Percolation Theory. Taylor & Francis, London and Philadelphia
22. Lárez-VC, Crescenzi V, Ciferri A (1995) Macromolecules 28:5280–5284
23. Cabane B, Lindell K, Engström S, Lindamn B (1996) Macromolecules 29: 3188–3197
24. Johansson HO, Karlström G, Tjerneld F (1993) Macromolecules 26:34478–4483
25. Takahashi SI, Fujimoto T, Miyamoto T, Inagaki H (1987) J Polym Sci: Part A Polym Chem 25:987–994
26. Miyamoto T, Long M, Donkai N (1995) Macromol Symp 99:141–147
27. Kato T, Yokoyama M, Takahashi A (1978) Colloid & Polym Sci 256:15–21
28. Nyström B, Walderhaug H, Hansen FK (1995) Langmuir 11:750–757
29. Michon C, Cuvelier G, Launay B (1993) Rheol Acta 32:94–103
30. San Biagio PL, Bulone D, Emanuele A, Madonia F, Di Stefano L, Giacomazza D, Trapanese M, Palma-Vittorelli MB, Palma MU (1990) Makromol Chem Macromol Symp 40:33–44
31. Luan CH, Parker TM, Gowda DC, Urry DW (1992) Biopolymers 32:1251–1261
32. Lewis KE, Robinson CP (1970) J Colloid Interface Sci 32:539–546
33. Chevillard C, Axelos MAV, to be published